

Dynamic Impact Factors for Simply-Supported Bridges Due to Vehicle Braking

by

Lu Deng, Fang Wang and Wei He

Reprinted from

Advances in Structural Engineering

Volume 18 No. 6 2015

Dynamic Impact Factors for Simply-Supported Bridges Due to Vehicle Braking

Lu Deng*, Fang Wang and Wei He

College of Civil Engineering, Hunan University, Changsha, Hunan 410082, China

(Received: 9 Jun 2014; Received revised form: 24 Sep 2014; Accepted: 24 Sep 2014)

Abstract: Previous studies have shown that the dynamic impact factors of bridges caused by vehicle braking may exceed those prescribed in the bridge design codes. While simple vehicle and bridge models were used in most of the previous studies, a three-dimensional vehicle-bridge coupled model was developed in this paper to study the dynamic impact factors for bridges due to vehicle braking. This model is able to deal with more complex bridge structures than most of the existing models in the literature and can produce more reasonable results. Considerable dynamic effects were observed on the bridge responses as well as on the contact forces between the bridge and the vehicle due to vehicle braking. The effects of several important parameters, including the vehicle braking position, deceleration rate, initial vehicle speed, and road surface condition, on the dynamic impact factors were studied. In addition, a comparison was made between the dynamic impact factors caused by vehicle braking and acceleration.

Key words: vehicle braking, dynamic impact factor, three-dimensional vehicle-bridge coupled model, inertial force.

1. INTRODUCTION

The dynamic response of bridges induced by moving vehicles, usually in terms of the dynamic impact factor, has been studied in considerable depth in the past. Different factors that influence the dynamic impact factor, such as vehicle speed, road surface condition (RSC), bridge span length and natural frequency, have been studied extensively (Chan *et al.* 2003; Brady *et al.* 2006; González *et al.* 2010; Li *et al.* 2006). However, in most of the published work, the vehicle was assumed to travel at a constant speed. Only a few studies were focused on the bridge responses caused by vehicle braking or acceleration. When a vehicle is subjected to braking, the vertical contact forces between the wheels of the vehicle and the bridge will experience significant changes due to a pitching moment, and significant bridge vibration can be induced (Lou 2005). Previous studies have shown that the resulting dynamic impact factors due to vehicle braking may exceed those

prescribed in the bridge design codes (Kishan and Traill-Nash 1977; Law and Zhu 2005; Ju and Lin 2007).

There have been a few studies on the effects of vehicle deceleration on the bridge responses. Kishan and Traill-Nash (1977) studied the vehicle braking effects on the response of a bridge which was idealized as a simply supported beam. Gupta and Traill-Nash (1980) presented some results on the impact factors due to the braking of a two-axle vehicle on a single-span bridge deck by using a ramped braking function. Mulcahy (1983) presented a method to study the dynamic responses of a single span multi-girder bridge due to vehicle braking using an orthotropic plate model for the bridge and a three-dimensional vehicle model. Yang and Wu (2001) investigated the behavior of a bridge under the effect of vehicle braking. In their study, the horizontal contact forces, i.e., friction forces, were calculated by multiplying the vertical contact forces by a friction coefficient. Later, Azimi *et al.* (2013)

*Corresponding author. Email address: denglu@hnu.edu.cn; Fax: +86-731-88822121; Tel: +86-731-88823320.

developed a modified two-dimensional vehicle-bridge interaction element which can account for vehicle deceleration with sliding. This model was an extension to the model developed by Yang and Wu (2001). It should be noted that the vehicle-bridge models developed in these two studies were mainly aimed for studying railway bridges. Law and Zhu (2005) studied the interaction between a three-axle truck and a bridge with a non-uniform cross-section. In their study, the vehicle was modeled as a group of moving loads with a fixed spacing, and the bridge was modeled as a multi-span continuous Benoulli-Euler beam. Ju and Lin (2007) developed a simple finite element model to simulate the vehicle-bridge interaction caused by the braking and acceleration of moving vehicles by adding horizontal springs and dampers into the vehicle model.

In most of the previous studies, however, simple bridge models (beam and plate models) were employed (Kishan and Trail-Nash 1977; Law and Zhu 2005; Ju and Lin 2007; Mulcahy 1983; Yang and Wu 2001; Azimi *et al.* 2013). Gupta and Traill-Nash (1980) showed that the dynamic impact factors obtained by using a plate model for the bridge were significantly smaller than those obtained by using a beam model. They concluded that a two-dimensional orthotropic plate or superior bridge model is necessary for analyzing vehicle-bridge interaction for bridge structures with certain complexity.

To achieve satisfactory accuracy for the dynamic impact factors obtained from numerical simulations as well as to be able to model more complex bridge structures, a three-dimensional vehicle-bridge coupled model was developed in this paper to study the bridge responses due to vehicle braking and acceleration. The effects of different factors, including the vehicle braking

position, deceleration rate, initial vehicle speed, and road surface condition, on the impact factors due to vehicle braking were investigated. A comparison was also made between the dynamic impact factors caused by vehicle braking and acceleration.

2. VEHICLE-BRIDGE COUPLED MODEL

2.1. Vehicle Model

In this study, a two-axle truck, as shown in Figure 1, was considered. The main parameters of the truck model are listed in Table 1, and more detailed information of this truck model is available in Xu and Guo (2003) and Zhang *et al.* (2006). This vehicle model is composed of a vehicle body and four wheels. The tires and suspension systems are idealized as linear elastic spring elements and dashpots. The vehicle body has five degrees of freedom (DOFs), including the translations in the y and z directions, rolling, yawing, and pitching. Each wheel has two DOFs, namely, the translations in the y and z directions. Therefore, this truck model has a total of 13 DOFs. It should be noted that the lateral DOFs were only aimed for future studies related to lateral contact forces and were not used in this study. A modal analysis was conducted on the vehicle model and the first five natural frequencies of the truck model are 1.147, 1.796, 1.940, 2.775, and 3.301 Hz, respectively, which agree with the results in Zhang *et al.* (2006).

2.2. Bridge Model

The bridge considered in this study is a simply-supported concrete slab-on-girder bridge which is a very common type of bridge in the United States. It was designed according to the LRFD design specification (AASHTO 2004). The bridge has a length of 24.38 m

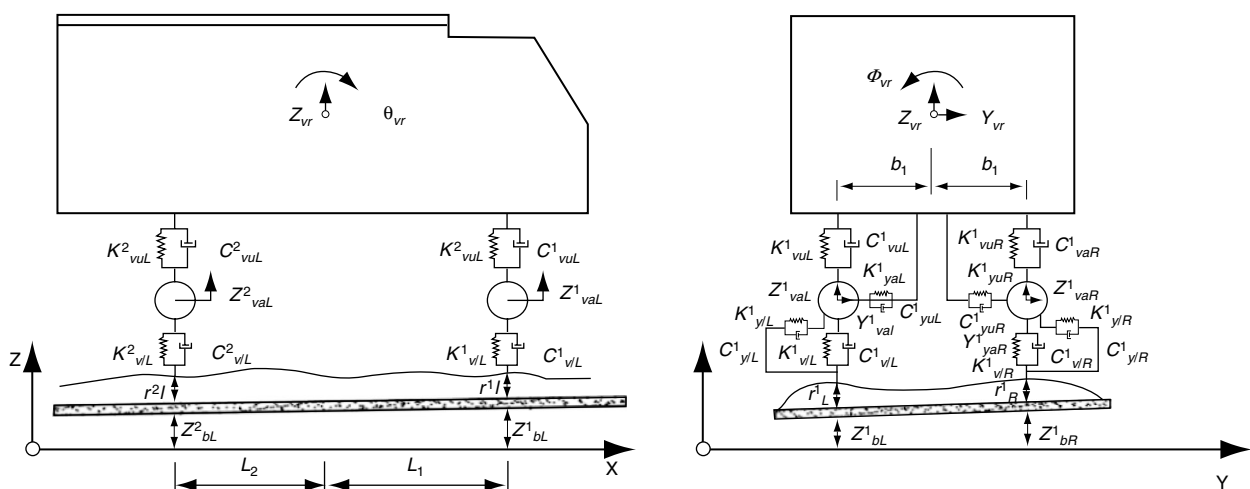


Figure 1. A two-axle vehicle model

Table 1. Major parameters of vehicle model

Parameters	Unit	Value
Total weight of vehicle	N	73,500
Mass of truck body	kg	4,500
Pitching moment of inertia of truck body	kg·m ²	5,483
Rolling moment of inertia of truck body	kg·m ²	1,352
Mass of each front axle suspension	kg	800
Mass of each front rear suspension	kg	700
Upper vertical spring stiffness for each axle	N/m	400,000
Upper lateral spring stiffness for each axle	N/m	300,000
Upper vertical damper coefficient for each axle	N·s/m	20,000
Upper lateral damper coefficient for each axle	N·s/m	20,000
Lower vertical spring stiffness for each axle	N/m	350,000
Lower lateral spring stiffness for each axle	N/m	120,000
Lower vertical damper coefficient for each axle	N·s/m	1,000
Lower lateral damper coefficient for each axle	N·s/m	1,000
Vehicle centroid height h_v	m	1.5
Distance L1	m	2.9
Distance L2	m	5.0
Distance b1	m	1.05

(80 ft), a roadway width of 9.75 m (32 ft), and a deck thickness of 0.20 m (8 in). It consists of five identical girders with a girder spacing of 2.13 m (7 ft). Figure 2 shows the cross-section of the bridge and the vehicle loading position. In the present study, the vehicle was set to travel along the centerline of the Lane 2. The bridge was modeled using solid elements (with three translational DOFs at each node) with the ANSYS program. Figure 3 shows the finite element model of

the bridge. The first five vibration modes of the bridge are described in Table 2 and the corresponding mode shapes are shown in Figure 4. A sensitivity study was conducted on the effect of number of modes on the accuracy of the simulated bridge responses. The simulated bridge deflection and strain at the mid-span of the bridge when the truck travels across the bridge at a speed of 0.5 m/s were compared to the static results obtained from the finite element analysis in the ANSYS program. It was found that the use of 20 modes can produce results with satisfactory accuracy with the maximum difference falling below 1%. Therefore, the first 20 bridge vibration modes were used in the numerical simulations.

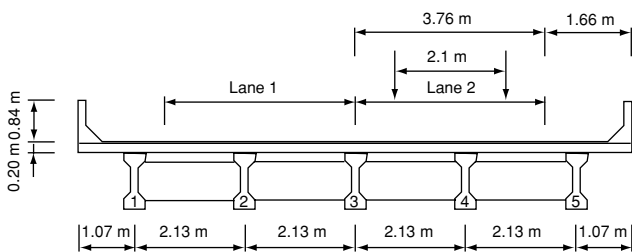


Figure 2. Bridge cross-section and vehicle loading position

2.3. Road Surface Condition

Road surface condition is known as a very important source of excitation for vehicle-induced bridge vibration. A road surface profile is usually assumed to be a zero-mean stationary Gaussian random process. A random road profile can be generated through an inverse Fourier transformation based on a power spectral density (PSD) function such as the one adopted in Dodds and Robson (1973):

$$r(X) = \sum_{k=1}^N \sqrt{2\varphi(n_k)\Delta n} \cos(2\pi n_k X + \theta_k) \quad (1)$$

where θ_k is a random phase angle which has a uniform distribution from 0 to 2π , $\varphi()$ is the PSD function ($\text{m}^3/\text{cycle}/\text{m}$) for the road elevation; and n_k is the wave number (cycle/m). The PSD function used by Huang

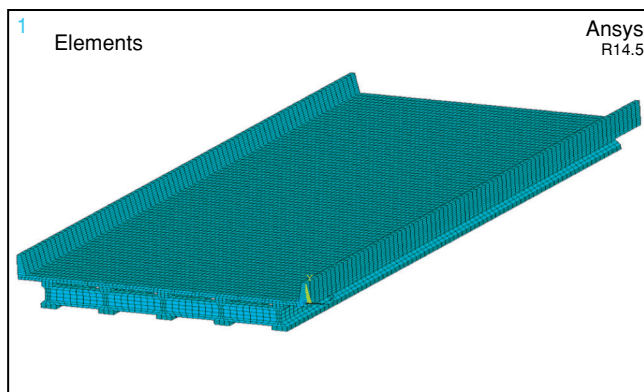


Figure 3. A finite element model for the bridge

Table 2. First five natural frequencies and corresponding mode shapes of the bridge

Mode number	Natural frequency (Hz)	Mode shape description
1	4.60	First vertical bending mode
2	6.23	First torsional mode
3	11.19	Second torsional mode
4	15.09	First lateral bending mode
5	16.29	Second vertical bending mode

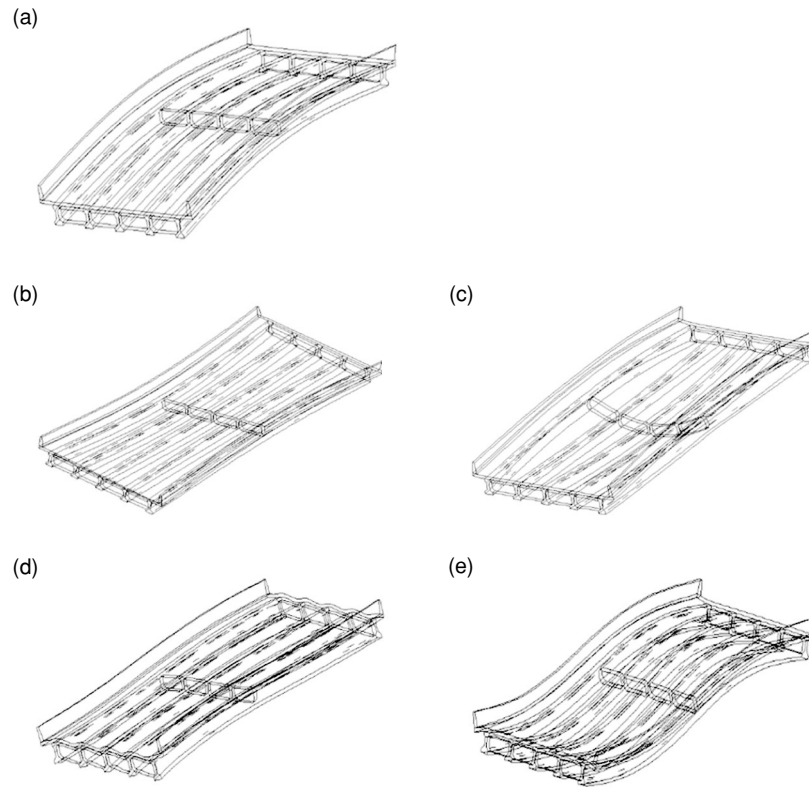


Figure 4. The first five mode shapes of the bridge: (a) mode 1; (b) mode 2; (c) mode 3; (d) mode 4 and (e) mode 5

and Wang (1993) was adopted in the present study, as shown below:

$$\varphi(n) = \varphi(n_0) \left(\frac{n}{n_0} \right)^{-2} \quad (n_1 < n < n_2) \quad (2)$$

where n is the spatial frequency (cycle/m), n_0 is the discontinuity frequency of $1/(2\pi)$ (cycle/m), $\varphi(n_0)$ is the roughness coefficient ($m^3/\text{cycle/m}$), n_1 and n_2 are the lower and upper cut-off frequencies, respectively.

Different road roughness indices are proposed by the International Organization for Standardization (ISO 1995). In this study, road surface conditions classified as “good”, “average”, and “poor” by the ISO were adopted. Sample road surface profiles are shown in Figure 5.

2.4. Equation of Motion of the Vehicle-Bridge Coupled System

For vehicles traveling at a constant speed, using the displacement relationship and the interaction force relationship at the contact points, the equation of motion of the vehicle-bridge coupled system can be established by combining the equations of motion of both the vehicle and the bridge, as shown below:

$$\begin{bmatrix} M_b \\ M_v \end{bmatrix} \begin{Bmatrix} \ddot{d}_b \\ \ddot{d}_v \end{Bmatrix} + \begin{bmatrix} C_b + C_{b-b} & C_{b-v} \\ C_{v-b} & C_v \end{bmatrix} \begin{Bmatrix} \dot{d}_b \\ \dot{d}_v \end{Bmatrix} + \begin{bmatrix} K_b + K_{b-b} & K_{b-v} \\ K_{v-b} & K_v \end{bmatrix} \begin{Bmatrix} d_b \\ d_v \end{Bmatrix} = \begin{Bmatrix} F_{b-r} \\ F_{b-r} + F_G \end{Bmatrix} \quad (3)$$

where C_{b-b} , C_{b-v} , C_{v-b} , K_{b-b} , K_{b-v} , K_{v-b} , F_{b-r} , and F_{b-r} are due to the vehicle-bridge interaction and are time-dependent terms.

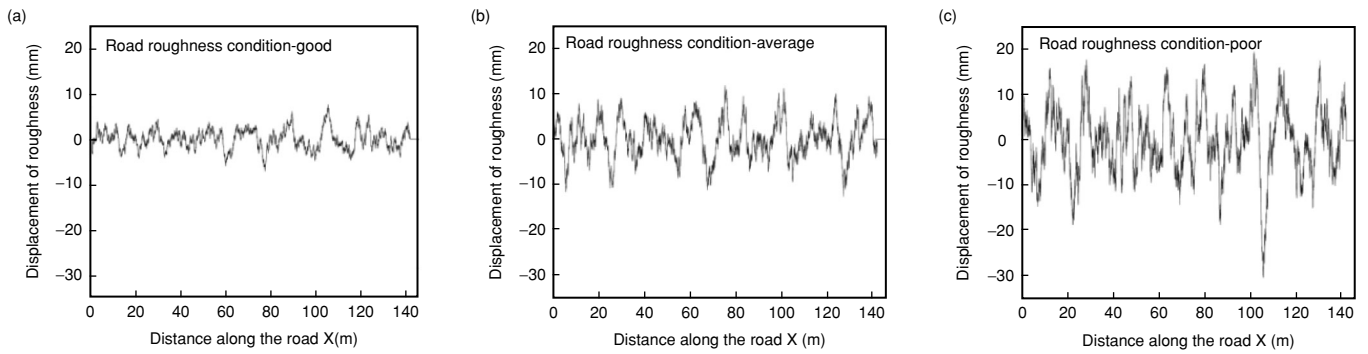


Figure 5. Sample road surface profiles: (a) good RSC; (b) average RSC and (c) poor RSC

The modal superposition technique was used in this study to simplify the equation of motion of the bridge, leading to significantly reduced computational effort. By doing this, Eqn 3 can then be simplified into the following:

$$\begin{aligned}
 & \begin{bmatrix} I \\ M_v \end{bmatrix} \begin{Bmatrix} \ddot{\xi}_b \\ \ddot{d}_v \end{Bmatrix} + \\
 & \begin{bmatrix} 2\omega_i \eta_i I + \Phi_b^T C_{b-b} \Phi_b & \Phi_b^T C_{b-v} \\ C_{v-b} \Phi_b & C_v \end{bmatrix} \begin{Bmatrix} \dot{\xi}_b \\ \dot{d}_v \end{Bmatrix} \\
 & + \begin{bmatrix} \omega_i^2 I + \Phi_b^T K_{b-b} \Phi_b & \Phi_b^T K_{b-v} \\ K_{v-b} \Phi_b & K_v \end{bmatrix} \\
 & \begin{Bmatrix} \xi_b \\ d_v \end{Bmatrix} = \begin{Bmatrix} \Phi_b^T F_{b-r} \\ F_{b-r} + F_G \end{Bmatrix} \tag{4}
 \end{aligned}$$

The fourth-order Runge-Kutta method was adopted to solve Eqn 4 in the time domain. For more details of the vehicle-bridge coupled system and the problem-solving process, readers can refer to Deng and Cai (2010).

When a vehicle traveling at a constant speed starts to brake or accelerate, the vehicle body tends to stay in the initial state of motion, resulting in a virtual force, usually called inertial force (or inertia), applied to the vehicle in the direction that is opposite to the change of vehicle speed. This inertial force can be calculated as:

$$F_1 = -ma \tag{5}$$

where m is the vehicle mass; a is the horizontal acceleration of the vehicle; and the minus sign denotes that the inertial force is in the opposite direction of acceleration. Most previous studies assumed a constant inertial force based on the deceleration rate during the vehicle braking process (Ju and Lin 2007; Azimi *et al.* 2013). In this study, constant deceleration or acceleration rates were assumed during the entire process and the inertial force was therefore constant during the entire process.

To slow down or speed up the vehicle, frictions between wheels and road surface (in the opposite direction to the inertia) will play as the external force. As a result, the inertial force, which acts on the mass centroid of the vehicle, and the friction forces acting on the contact surfaces of the vehicle will form a pitching moment. This pitching moment will result in a pitching motion of the vehicle that can be easily sensed by the driver and passengers. The pitching moment is formulated as:

$$M = F_l h_v \tag{6}$$

where h_v is the height of the mass centroid of the vehicle from the road surface level. An existing vehicle-bridge coupled system developed to deal with constant vehicle speeds (Deng and Cai 2010) was modified to incorporate the effects of vehicle speed change. Numerical simulations were conducted based on this modified system and the results will be presented in the following.

3. NUMERICAL STUDIES

3.1. Problem Description

The dynamic impact factor is defined as the increment of static vehicle load effect due to the dynamic vehicle loads and is usually calculated as follows:

$$IM = \frac{R_{dyn} - R_{sta}}{R_{sta}} \tag{7}$$

where R_{dyn} and R_{sta} are the maximum dynamic and static responses of the bridge, respectively. In the present study, the deflection and strain at the midspan of the girder carrying the largest amount of vehicle load were selected as the bridge responses for calculating the impact factors. The maximum static responses were obtained from a case in which the vehicle was set to cross the bridge at a crawling speed. The obtained maximum static responses

were also verified against the results obtained from a static analysis using the ANSYS program.

In the present study, the vehicle-bridge interaction analysis was run 20 times with 20 randomly generated road surface profiles under the given road surface condition. Then, the average value of the 20 impact factors was obtained. Twenty impact factors were considered to be enough based on a statistic analysis which shows that the variation of the estimated mean of the impact factors can be controlled within a satisfactory range with 20 impact factors considered (Liu *et al.* 2002; Deng and Cai 2010).

In the following sections, numerical simulations will be presented as follows: the bridge responses at the midspan and the contact forces are firstly investigated. Then, the influences of different parameters, including the vehicle braking position, deceleration rate, initial vehicle speed, and road surface condition, on the impact factors are studied. Finally, a comparison will be made between the effects of vehicle braking and acceleration on the impact factors. It should be pointed out that the position of vehicle refers to the position of the front wheels in the longitudinal direction and the braking position refers to the position of vehicle when starting to brake hereafter.

3.2. Bridge Responses at Midspan

In this series of case studies, the truck was set to travel at an initial speed of 20 m/s and to start deceleration when the front wheels reached the “L/8” position, i.e., the one-eighth span position on the bridge. A random road surface profile, which is classified as “good” according to ISO, was used. Three different deceleration rates within a reasonable range, namely, $a = -2 \text{ ms}^{-2}$, $a = -4 \text{ ms}^{-2}$, and $a = -6 \text{ ms}^{-2}$, were studied. These deceleration rates were also adopted in the studies by Law and Zhu (2005) and Azimi *et al.* (2013). In the following section, the bridge responses obtained from the cases with these three deceleration rates will be compared to the results from the case with the vehicle traveling at a constant speed.

The bridge responses at the midspan, including deflection, strain, and vertical acceleration, under different deceleration rates are plotted in Figure 6. The corresponding maximum static displacement (-0.753 mm) and strain ($8.82 \mu\epsilon$) are also plotted in Figures 6(a) and (b) for the purpose of comparison. It should be noted that the results from the runs with $a = -4 \text{ ms}^{-2}$ are not included in the plots in order to improve the readability of the figures.

As can be seen from the comparison between the bridge accelerations for the three cases in Figure 6(c),

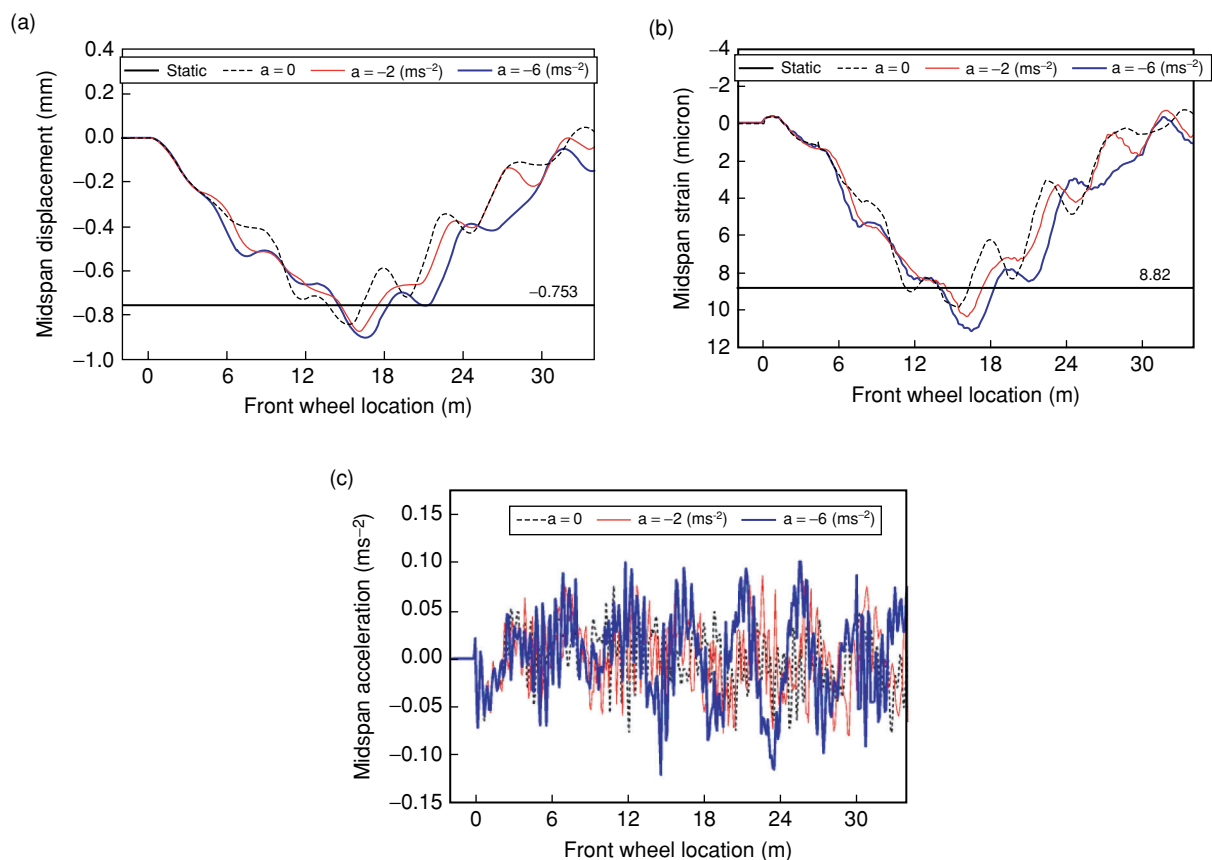


Figure 6. Bridge responses at midspan with and without vehicle braking effect: (a) displacement; (b) strain and (c) acceleration

bridge vibration becomes more significant as the magnitude of deceleration increases. From Figures 6(a) and (b), it is obvious to see that the maximum bridge deflection and strain increase as the magnitude of deceleration increases although bridge deflection and strain may not be as sensitive to vehicle braking as acceleration.

3.3. Contact Forces

Figure 7 shows results of the simulated vertical contact forces for the front and rear wheels under three cases, i.e., vehicle traveling at a constant speed and braking with deceleration rates of -2 ms^{-2} and -6 ms^{-2} , respectively. As described previously, an initial speed of 20 m/s was used and the vehicle was set to brake at the “L/8” position. The static vertical contact forces are also plotted as a reference.

As can be expected, significant interactions were induced by vehicle braking, which can be seen from the oscillation of contact forces. Moreover, the oscillation becomes stronger as the magnitude of deceleration increases. In addition, the contact forces of the front wheels increase and the contact forces of the rear wheels decrease due to the pitching moment. Similar trends in the change of

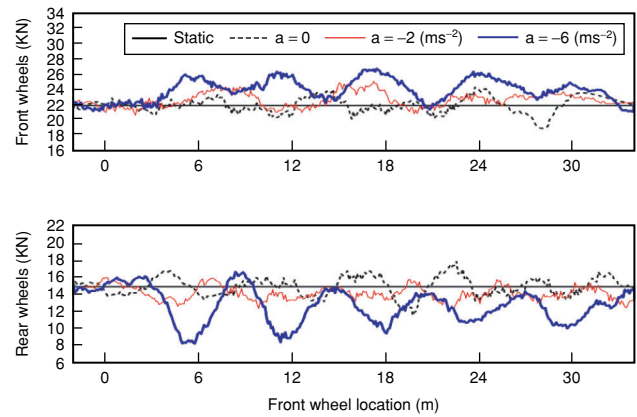


Figure 7. Contact forces for front and rear wheels (braking case)

wheel contact forces were also observed in previous studies (Law and Zhu 2005; Azimi *et al.* 2013).

3.4. Parametric Studies

3.4.1. Vehicle braking position

The impact factors obtained from the seven different braking positions with the three different deceleration rates are plotted in Figure 8. The vehicle was set to travel

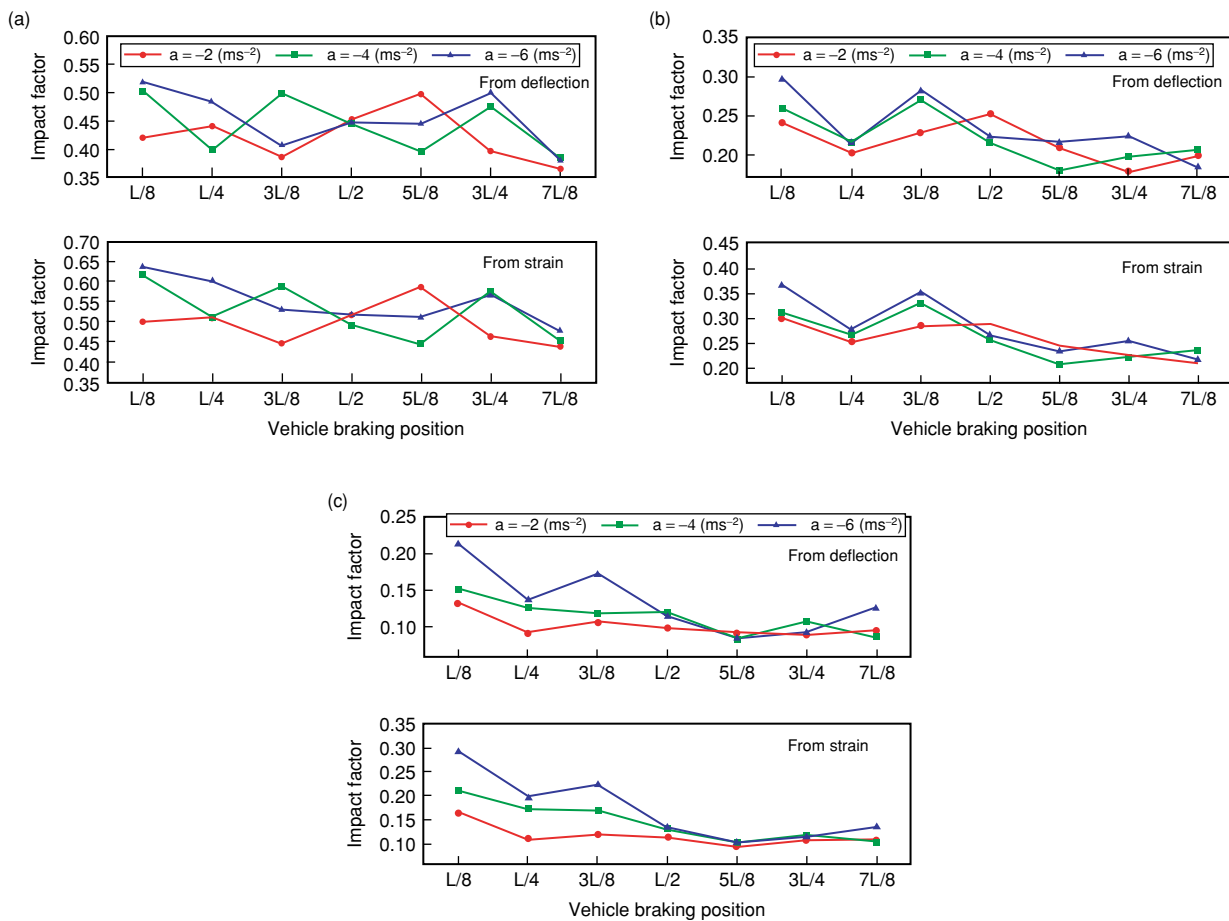


Figure 8. Impact factors under different deceleration rates and braking positions: (a) poor RSC; (b) average RSC and (c) good RSC

at an initial speed of 20 m/s. Figures 8(a)~(c) represent the results for poor, average, and good road surface conditions, respectively. It can be seen that in most cases braking at the “L/8” position produces larger impact factors compared with braking at other positions. These results are generally consistent with the findings by other researchers. Gupta and Traill-Nash (1980) found that the maximum dynamic impact factors were obtained when the vehicle started braking within the first half span of the bridge while Law and Zhu (2005) found that the maximum dynamic impact factors were obtained when the vehicle braked within the first quarter span. It can also be observed that the impact factors calculated from strain are in general larger than those calculated from deflection. While different observations were also reported by some other researchers (Paultre *et al.* 1992; Law and Zhu 2005; Szurgott *et al.* 2010), no consensus has yet been reached.

3.4.2. Vehicle initial speed and deceleration rate

Five initial vehicle speeds ranging from 10 m/s to 30 m/s with intervals of 5 m/s were considered. The vehicle

braking position was set to “L/8” for all cases. Figures 9(a)~(c) show the impact factors for different deceleration rates when the vehicle was set to travel at the five different initial speeds under the three different road surface conditions, respectively. It can be seen from Figure 9 that the trend of variations of the impact factors with respect to the initial vehicle speed are difficult to predict; however, the trends are generally consistent with the trends when the vehicle was traveling at a constant speed (Brady *et al.* 2006; Deng and Cai 2010). It can also be observed from the three figures that the increase of the magnitude of deceleration rate generally results in an increase of impact factors. It is worth noting that under a deceleration rate of -6 ms^{-2} , in a large portion of cases the resulting dynamic impact factors can be greater than those under constant vehicle speeds by 0.1 or even more.

3.4.3. Road surface condition

The dynamic impact factors for the deceleration rate of -4 ms^{-2} are plotted against the initial vehicle speed in Figure 10 for the three road surface conditions

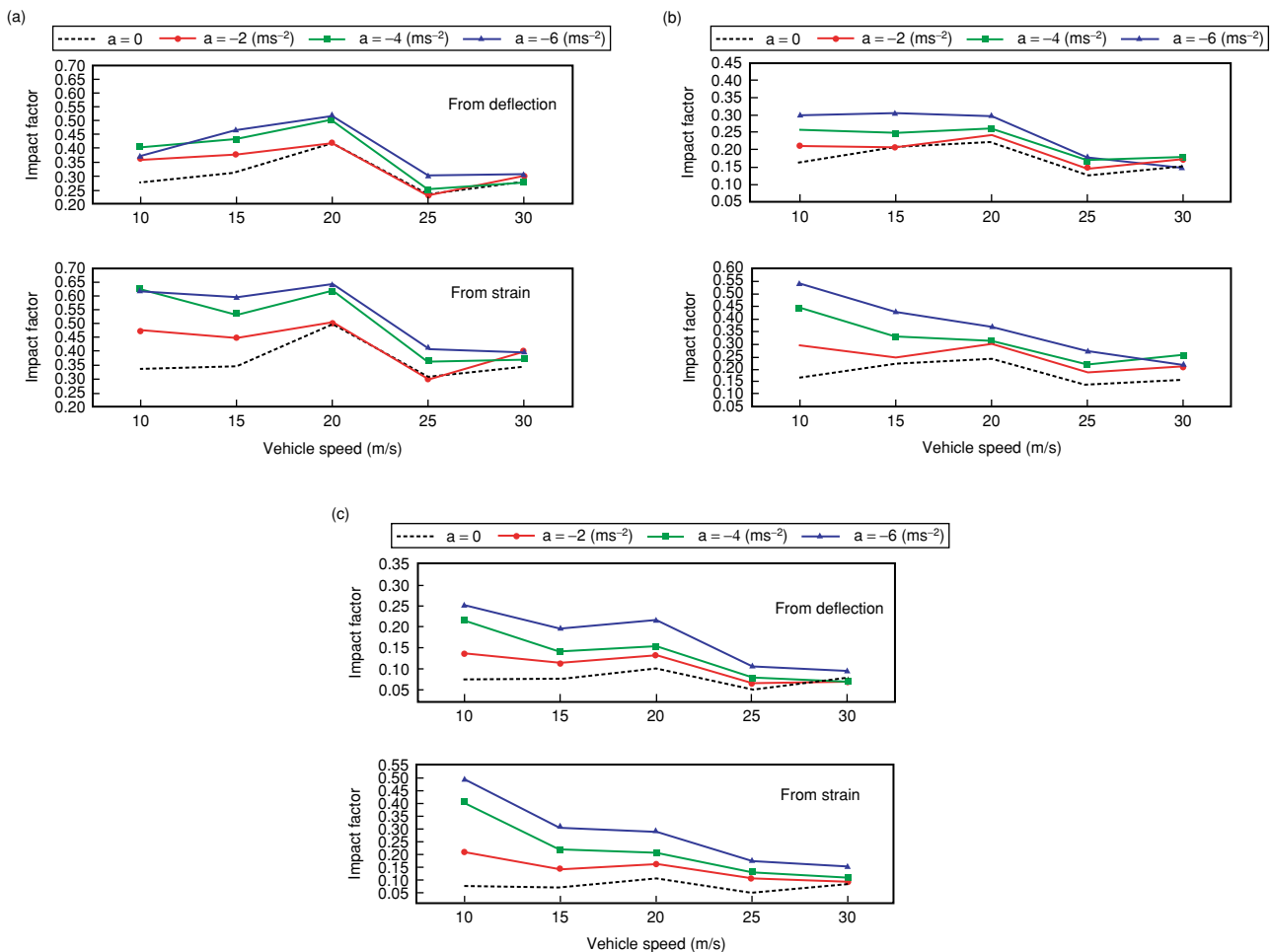


Figure 9. Impact factors under different vehicle initial speeds and deceleration rates: (a) poor RSC; (b) average RSC and (c) good RSC

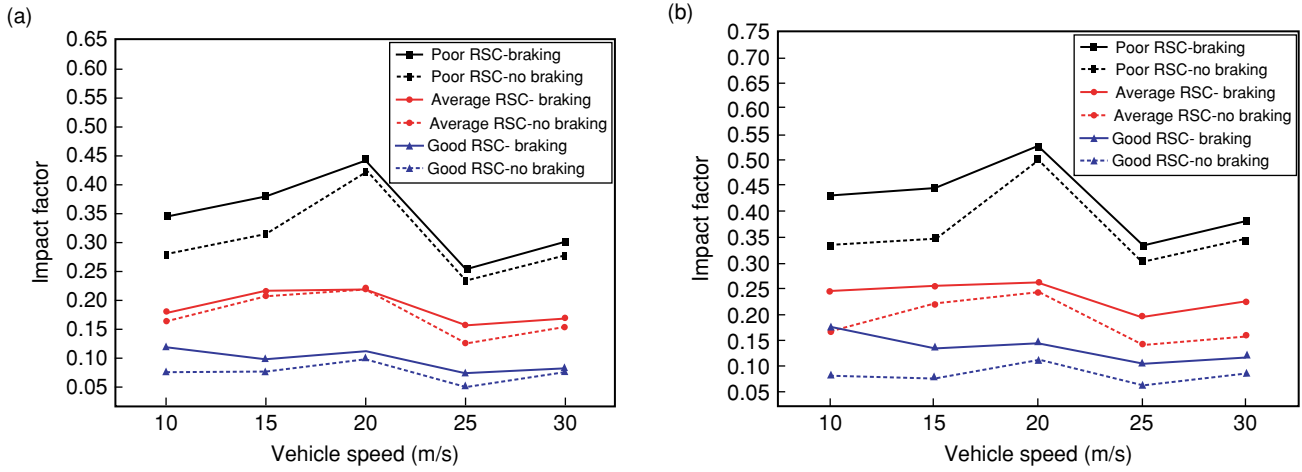


Figure 10. Impact factors under different road surface conditions: (a) from deflection and (b) from strain

considered. The results for the runs with constant speeds are also included for comparison. It should be noted that in order to reduce the bias due to limited data from one case, the results presented in Figure 10 are the average dynamic impact factors for all seven vehicle braking positions. As can be seen from Figure 10, the average impact factors vary from greater than 0.5 when the road surface condition is poor to less than 0.10 when the road surface condition is good, indicating that the road surface condition has a significant influence on the impact factors, which is similar to the influence of road surface condition under the cases with a constant vehicle speed (Liu *et al.*2002; Li *et al.* 2006; Deng and Cai 2010). From the figures, it is also observed that the impact factors due to vehicle braking are in general greater than those without vehicle braking effects with the largest difference reaching 0.1, which agrees with the finding in the previous section.

It should be noted that while the dynamic impact factors all fall below the value of 0.33 prescribed in the LRFD design specification (AASHTO 2004) under average and good road surface conditions, a large portion of the impact factors exceed 0.33, especially for those calculated from deflection or strain under poor road surface condition. This portion could become even larger when the vehicle started braking at the “L/8” position, as shown in Figure 8. Law and Zhu (2005) also concluded that under poor road surface condition, the resulting dynamic impact factors can be significantly larger than those adopted in the bridge design codes.

3.4.4. Braking vs. acceleration

For the acceleration case, the inertial force is applied in the direction opposite to that for the braking case. Figure 11 shows the contact forces with acceleration

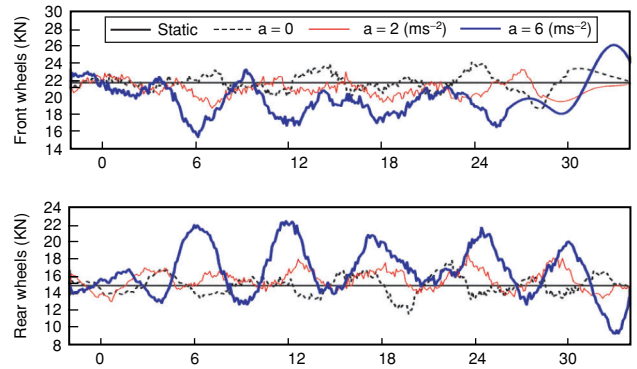


Figure 11. Contact forces for front and rear wheels (acceleration case)

rates of 2 ms⁻² and 6 ms⁻² for the front and rear wheels, respectively. The vehicle was set to travel at an initial speed of 20 m/s and to start acceleration when the front wheels reached the “L/8” position. The results from the run with a constant speed are also included for comparison. It can be observed that due to vehicle acceleration effect, the contact forces for the front wheels decrease while the contact forces for the rear wheels increase, showing an opposite trend to the vehicle braking case. Also, the dynamic effects increase significantly as the acceleration rate increases from 2 ms⁻² to 6 ms⁻².

Figure 12 shows the impact factors for different vehicle braking and acceleration positions under good road surface condition. The results for different speed change rates are presented separately. It can be observed that the impact factors for the acceleration cases generally vary in an opposite fashion to that for the braking cases: larger impact factors are obtained when the vehicle starts acceleration within the second half

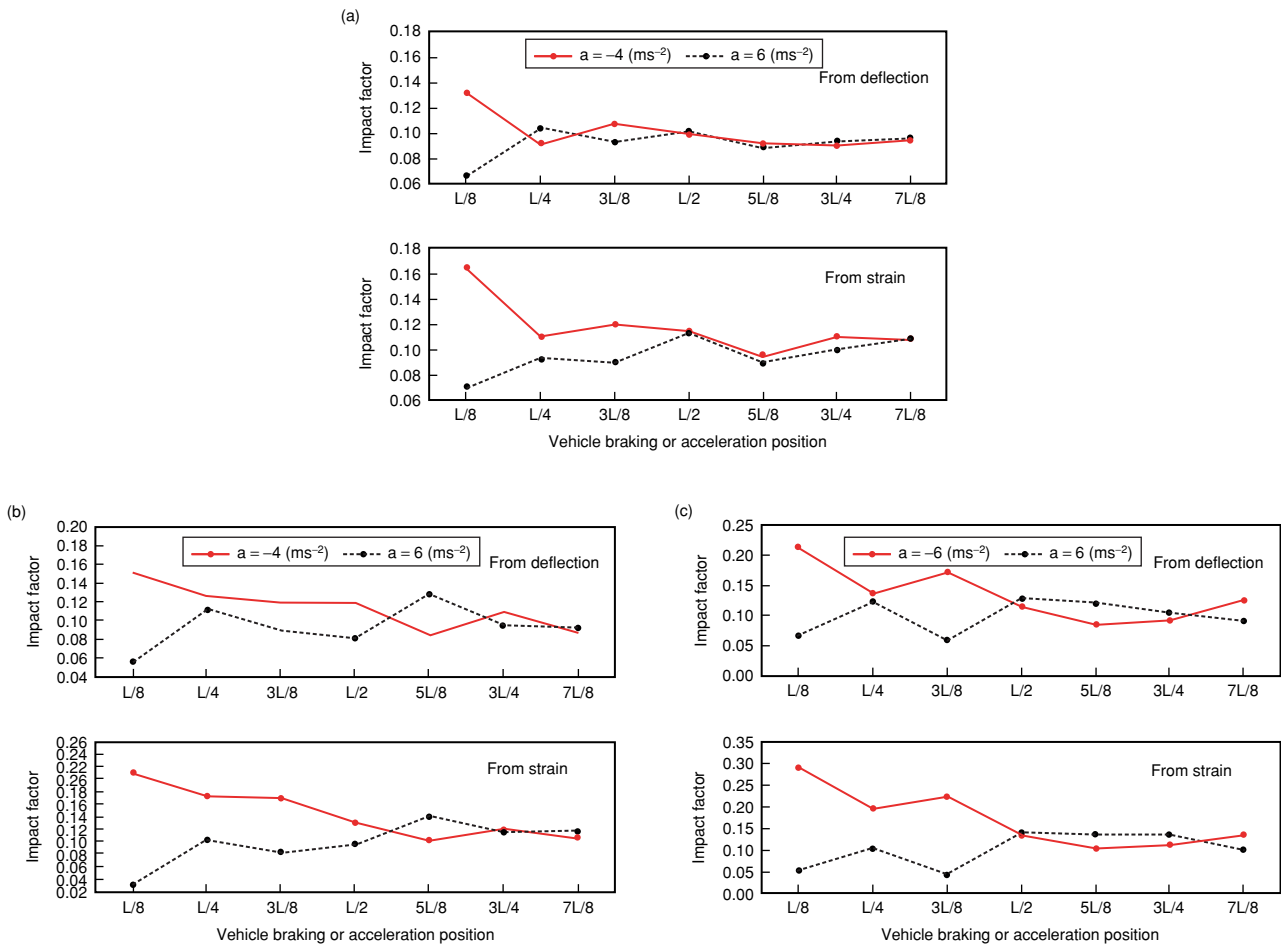


Figure 12. Impact factors under different braking and acceleration positions

span of the bridge. The figures also reveal that the impact factors obtained from the acceleration cases are in general smaller than those from the braking cases even though the magnitudes of acceleration and deceleration are the same.

4. CONCLUSIONS

In this study, a three-dimensional vehicle-bridge coupled model was developed to study the dynamic responses of a simply-supported bridge due to vehicle braking. The effects of vehicle braking on the bridge responses and the contact forces were first studied. Parametric studies were then conducted to study the effects of several important parameters, including the vehicle braking position, deceleration rate, initial vehicle speed, and road surface condition, on the dynamic impact factor. A comparison between the effects of braking and acceleration was also made. Based on the results from the numerical simulations, the following conclusions can be reached:

(1) In general, vehicle braking causes much larger dynamic impact factors than vehicle traveling at a

constant speed. With a vehicle deceleration rate of -6 ms^{-2} , this difference can be as large as 0.1.

- (2) For the bridge studied, braking within the first quarter span causes larger impact factors in comparison to braking at other positions. In contrast, accelerating within the second half span produces larger impact factors than accelerating within the first half span.
- (3) The influence of initial vehicle speed on the impact factors is unclear; however, the trend of variation of impact factors with respect to the initial vehicle speed is generally consistent with the trend under the cases with constant vehicle speeds.
- (4) Within the range of deceleration rate studied (0 to -6 ms^{-2}), an increase in the magnitude of deceleration generally leads to an increase of the dynamic impact factors.
- (5) Road surface condition has a significant influence on the impact factors. Under poor road surface condition, vehicle braking can cause significant dynamic effects even when the vehicle travels at a low initial speed.

- (6) For the bridge studied, the impact factors obtained from strain are in general larger than those obtained from deflection. However, it should be noted that different conclusions have been reported under different circumstances by other researchers.

ACKNOWLEDGEMENTS

This work was supported by the National Natural Science Foundation of China (Grant No. 51208189 and No. 51478176) and Excellent Youth Foundation of Hunan Scientific Committee (Grant No. 14JJ1014).

REFERENCES

- AASHTO (2004). *AASHTO LRFD Bridge Design Specifications*, American Association of State Highway and Transportation Officials (AASHTO), Washington D.C., USA.
- Azimi, H., Galal, K., and Pekau, O.A. (2013). "A numerical element for vehicle-bridge interaction analysis of vehicles experiencing sudden deceleration", *Engineering Structures*, Vol. 49, pp. 792–805.
- Brady, S.P., O'Brien, E.J. and Žnidarič, A. (2006). "Effect of vehicle velocity on the dynamic amplification of a vehicle crossing a simply supported bridge", *Journal of Bridge Engineering*, ASCE, Vol. 11, No. 2, pp. 241–249.
- Chan, T.H.T., Yu, L., Yung, T.H. and Chan, J.H.F. (2003). "A new bridge-vehicle system Part II: Parametric Study", *Structural Engineering and Mechanics*, Vol. 15, No.1, pp. 21–38.
- Dodds, C. and Robson, J. (1973). "The description of road surface roughness", *Journal of Sound and Vibration*, Vol. 31, No. 2, pp. 175–183.
- Deng, L. and Cai, C.S. (2010). "Development of dynamic impact factor for performance evaluation of existing multi-girder concrete bridges", *Engineering Structures*, Vol. 32, No. 1, pp. 21–31.
- Gupta, R. and Traill-Nash, R. (1980). "Bridge dynamic loading due to road surface irregularities and braking of vehicle", *Earthquake Engineering & Structural Dynamics*, Vol. 8, No. 2, pp. 83–96.
- González, A., O'Brien, E.J., Cantero, D., Li, Y., Dowling, J. and Žnidarič, A. (2010). "Critical speed for the dynamics of truck events on bridges with a smooth road surface", *Journal of Sound and Vibration*, Vol. 329, No. 11, pp. 2127–2146.
- Huang, D., Wang, T.L. and Shahawy, M. (1993). "Impact studies of multi-girder concrete bridges", *Journal of Structural Engineering*, ASCE, Vol. 119, No. 8, pp. 2387–2402.
- ISO (1995). *Mechanical Vibration-Road Surface Profiles-Reporting of Measured Data*, ISO 8068: 1995 (E), International Organization for Standardization, Geneva, Switzerland.
- Ju, S.H. and Lin, H.T. (2007). "A finite element model of vehicle-bridge interaction considering braking and acceleration", *Journal of Sound and Vibration*, Vol. 303, No. 1, pp. 46–57.
- Kishan, H. and Traill-Nash, R.W. (1977). *A Modal Method for Calculation of Highway Bridge Response with Vehicle Braking*, Civil Engineering Transactions, Institution of Engineers, Australia.
- Law, S.S. and Zhu, X.Q. (2005). "Bridge dynamic responses due to road surface roughness and braking of vehicle", *Journal of Sound and Vibration*, Vol. 282, No. 3–5, pp. 805–830.
- Li, Y., O'Brien, E.J. and González, A. (2006). "The development of a dynamic amplification estimator for bridges with good road profiles", *Journal of Sound and Vibration*, Vol. 293, No. 1–2, pp. 125–137.
- Liu, C., Huang, D. and Wang, T.L. (2002). "Analytical dynamic impact study based on correlated road roughness", *Computers & Structures*, Vol. 80, No. 20, pp. 1639–1650.
- Lou, P. (2005). "A vehicle-track-bridge interaction element considering vehicle's pitching effect", *Finite Elements in Analysis and Design*, Vol. 41, No. 4, pp. 397–427.
- Mulcahy, N.L. (1983). "Bridge response with tractor-trailer vehicle loading", *Earthquake Engineering & Structural Dynamics*, Vol. 11, No. 5, pp. 649–665.
- Paultre, P., Chaallal, O. and Proulx, J. (1992). "Bridge dynamics and dynamic amplification factors-a review of analytical and experimental findings", *Canadian Journal of Civil Engineering*, Vol. 19, No. 2, pp. 260–278.
- Szurgott, P., Wekezer, J., Kwasniewski, L., Siervogel, J. and Ansley, M. (2010). "Experimental assessment of dynamic responses induced in concrete bridges by permit vehicles", *Journal of Bridge Engineering*, ASCE, Vol. 16, No. 1, pp. 108–116.
- Xu, Y.L. and Guo, W.H. (2003). "Dynamic analysis of coupled road vehicle and cable-stayed bridge systems under turbulent wind", *Engineering Structures*, Vol. 25, No. 4, pp. 473–486.
- Yang, Y.B. and Wu, Y.S. (2001). "A versatile element for analyzing vehicle-bridge interaction response", *Engineering Structures*, Vol. 23, No. 5, pp. 452–469.
- Yin, X.F., Fang, Z., Cai, C.S. and Deng, L. (2010). "Non-stationary random vibration of bridges under vehicles with variable speed", *Engineering Structures*, Vol. 32, No.8, pp. 2166–2174.
- Zhang, Y., Cai, C.S, Shi, X. and Wang, C. (2006). "Vehicle-induced dynamic performance of FRP versus concrete slab bridge", *Journal of Bridge Engineering*, ASCE, Vol. 11, No. 4, pp. 410–419.